S.V. Mamykin, I.B. Mamontova, N.V. Kotova, O.S. Kondratenko, T.R. Barlas, V.R. Romanyuk, P.S. Smertenko, N.M. Roshchina

Nanocomposite Solar Cells Based on Organic/Inorganic (Clonidine/Si) Heterojunction with Plasmonic Au Nanoparticles

V.E. Lashkaryov Institute of Semiconductor Physics National Academy of Sciences of Ukraine, Kyiv, Ukraine,
mamykin@isp.kiev.ua

The peculiarities of optical and electrical properties of organic(clonidine)/inorganic(Si) heterojunction with plasmonic Au nanoparticles have been investigated by reflection spectra, photoelectric and current-voltage characteristics measurements. Porous nanostructured surfaces of silicon wafers were obtained by the method of selective chemical etching initiated by metal (gold) nanoparticles. Nanocomposites based on nanostructured silicon, clonidine and gold nanoparticles have been made. Two types of structure, namely, solar cells and photodiodes on the basis of such heterojunction were analysed. The reflection spectra of light confirmed the excitation of the plasmon mode in nanocomposites with gold nanoparticles. Photoelectric studies have shown an increase of the photocurrent of solar cells obtained as a result of using both nanostructured silicon and gold nanoparticles in 1.5 and 7 times, respectively. Study of the injection properties of the structures showed that the clonidine layer always facilitates the injection of current carriers, while gold nanoparticles limit the current in the case of a flat surface.

Keywords: nanocomposite; organic/inorganic heterojunction; silicon; gold nanoparticles; clonidine; electron and hole injection; dimensionless sensitivity; solar cell.

Introduction

Nanocomposite materials for photovoltaic purposes have been used for a long time [1-6]. The first works by Fujishima and Honda [1], which investigated the photoelectric effect in samples where a key element was a layer of titanium dioxide nanoparticles, were published in the 1970s. The low efficiency of such elements, due to the high bandwidth in TiO_2, which can absorb only the blue and UV part of the solar spectrum, is enhanced by the introduction of an additional component in the composite – dye sensitizers [7, 8] with a wide range of absorption of the visible and near-infrared spectrum, sufficiently resistant to oxidation and with suitable energy parameters of the HOMO/LUMO (highest filled molecular orbital/lowest molecular orbital) position, so that the LUMO level is higher (>0.3 eV) than the level of the conduction band TiO_2 (acceptor) and the electrons generated in the sensitizer (donor) could pass without barrier to the acceptor (Fig. 1). The HOMO level should be close enough to the LUMO to absorb a significant part of the solar spectrum, but also to provide a sufficient level of generated voltage. The optimum energy distance between HOMO and LUMO is 1.3 - 1.4 eV for single junction solar cells (SC). The above mentioned dyes [9], conductive polymers [10, 11] and nanoparticles of another (CdSe, CdTe, CdS [12], PbS, PbSe [13, 14]) semiconductors with a lower band gap may play the role of donors in such SCs. On the other hand, the transport properties of the acceptor can be improved by selecting a suitable material. Carbon nanomaterials – chemically modified fullerenes [15], nanotubes [16], graphene [17], and ZnO, SnO, CrO_x, CuO, WO_3 [18] are used. Moreover, with a sufficiently low bandwidth, they act not only as electron acceptors, but also contribute to the photoconversion by generating their electron-hole pairs. The semiconductors that have the best charge transport characteristics are Si, InP, and GaAs, where the electron
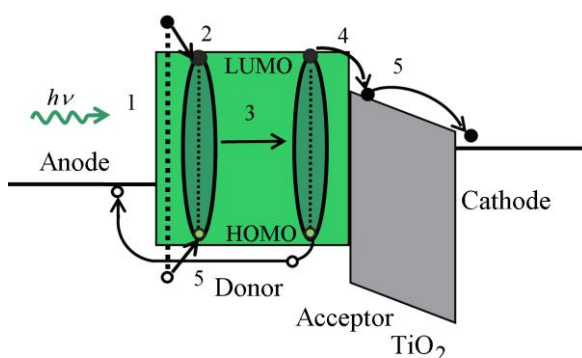
Fig. 1. Schematic representation of the hybrid solar cell's energy diagram and the processes taking place: absorption of photons in the donor (1), generation of excitons (2), diffusion of excitons into the heterojunction region (3), dissociation of excitons (4), transport of carriers (electrons in the acceptor and holes in the donor) (5).

mobility values are ~1000, ~8000, ~5000 cm^2/(Vs), respectively. Attempts to create hybrid SCs were also made on their basis. Thus, the structure based on the P3HT/GaAs heterojunction [19] showed an efficiency of ~1.5 %, the efficiency of the structure of quercetin/p-InP was ~0.1 % [20]. A very promising type of such SC is the heterojunction between the organic film PEDOT:PSS and Si, where the efficiency of 14.8 % [21], 15.5 % [22] and 17.4 % [23] has already been achieved.

One of the major problems in such composite hybrid solar cells is the charge transport, which is primarily due to the properties of organic component. Except of perovskites (a unique class of semi-organics), they generally have a short (~20 nm) diffusion length of excitons excited by light. It is difficult for them to reach the heterojunction region where charge separation occurs. This leads to the need to use very thin layers (<100 nm) of organics, which results in low light absorption by such layers. One way to increase this absorption is to use microrelief heterojunctions, porous layers, where light is scattered and captured by multiple reflections [24]. The use of plasmon-active metal Au, Ag, Cu nanoparticles of 20 - 100 nm in size [25] is also promising way to increase light absorption. They have a cross-section of light scattering significantly larger than their diameter (up to 10 times). A significant increase in the electromagnetic field and increase the time of light interaction with matter occurs near metal nanoparticles (NPs). As a result, light absorption in the composite is significantly enhanced with a relatively small number of nanoparticles. Since it is a metal, the conductivity of the composite is also increased.

The problem remains the search and synthesis of organic donors with HOMO/LUMO levels suitable for specific acceptor, optimization of heterojunction design, morphology and electronic properties of the acceptor. One of the promising organic donors is N-(2,6-dichlorophenyl)-4,5-dihydro-1H-imidazol-2-amine (clonidine). Its properties as a donor layer in the heterojunction with bulk silicon were studied in [26]. SCs of this type with a pyramidal microrelief had an

efficiency of 8 % which is not enough for their commercial use. In this work we propose to use a porous layer of a semiconductor with plasmon-active metal nanoparticles as a component of a heterojunction with clonidine. The advantage of such a structure is the large contact area, which will facilitate the collection and transport of carriers. Nanostructured semiconductors, due to the quantum-size effect, allow the band gap to be altered (enlarged) [27, 28], so one can choose the optimum for contact with a particular donor. In addition, it can be noted that the use of metal-assisted chemical etching for the fabrication of a porous layer should not change the concentration of the main carriers and the conductivity of the material unlike to electrochemical etching where the depletion region is formed after pores creation.

The aim of this work is to study the possibility of increasing the efficiency of clonidine/Si solar cells using nanocomposite based on porous silicon, clonidine and plasmon-active metal (Au) nanoparticles.

I. Materials and methods

The properties of N-(2,6-dichlorophenyl)-4,5-dihydro-1H-imidazol-2-amine (clonidine) as a donor layer in a bulk silicon heterojunction were investigated in [26], where the obtained SC showed efficiency about 8 %. The structure of the clonidine molecule is shown in Fig. 2a. It consists of a benzene ring with double bonds between carbon atoms that form a conductive electron that can move from molecule to molecule. This has led to some conductivity of clonidine films and its "semiconductor" properties.

The generalized structure of SCs proposed in the work is presented in Fig. 2b. It consists of nanocomposite based on a donor N-(2,6-dichlorophenyl)-4,5-dihydro-1H-imidazol-2-amine (clonidine) deposited on a layer of
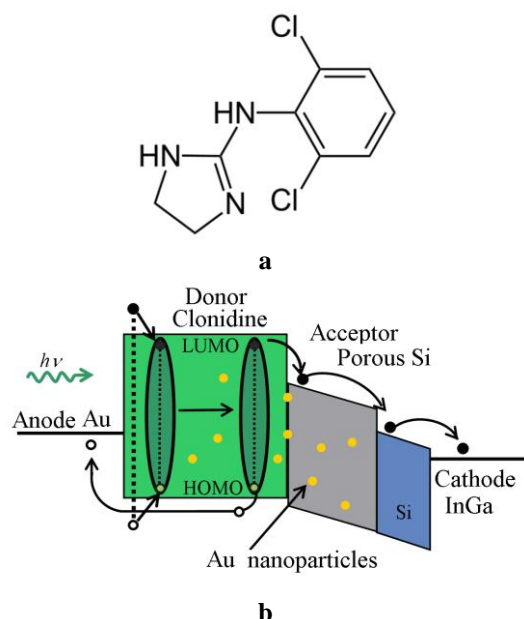

a

b

Fig. 2. Structure of a clonidine molecule (*a*) and generalized energy diagram of studied hybrid solar cells (*b*).

porous material (porous Si) with embedded plasmon-active metal (Au) nanoparticles on a semiconductor (Si) substrate. The structure is completed by top Au contact of greed type and bottom ohmic InGa contact to Si substrate.

Surface nanocomposite layers were fabricated on the basis of porous silicon with embedded gold nanoparticles produced with metal-assisted chemical etching (MACE) [29]. In this method, the morphologies of the resulting etched structures would usually be defined by the shape and size of the preliminary deposited metal catalyst. Usually, straight pores are form if isolated Ag or Au particles are used to assist the etching of a Si substrate. Well-separated noble metal particles commonly result in well-defined pores. Electroless deposition is a simple method for the deposition of noble metal island film of controlled morphology. Polished silicon single crystal wafer (100) *n*-type conductivity, doped with phosphorus with a resistivity of 0.5-2.4 ohm·cm was used as a substrate. Pre-cleaning of silicon wafers was carried out in ammonia-peroxide aqua solution. Native silicon oxide was removed in 10% HF solution immediately before the deposition of metal nanoclusters. Au nanoclusters on the surface of Si were grown by photoinduced chemical deposition (called also as electroless deposition) from an aqueous solution of $AuCl_3$ salt [30] with concentration of Au^{3+} ions of 0.5-1 g/l. To obtain metal film with narrow size distributed and isolated islands the deposition time 7 min was used. These nanoclusters were used as catalyst for the chemical etching of pores in silicon wafer with $H_2O_2:HF:H_2O$ (1:2:10) solution at room temperature for t=1-5 min. As a result of metal-assisted etching, pores of the appropriate size 10-20 nm were formed in silicon, at the bottom of which are these metal nanoparticles. Since further studies also required for comparison the SCs on textured silicon surface without gold nanoparticles, several samples were treated for 2 minutes in a solution of $KI:I_2:H_2O$ (4 g:1 g:40 ml) to dissolve and remove a gold from pores.

Clonidine films were deposited by prolonged exposure of flat and porous silicon substrates in aqueous clonidine solutions at room temperature.

Electron microscopy investigations of porous substrate surfaces were performed with JSM-6700F (JEOL) scanning electron microscope.

Nanocomposites based on porous Si and Au NPs were characterized by spectroscopic ellipsometry and reflectometry of polarized light in the visible and near-IR range. Spectroscopic ellipsometer SE-2000 (Semilab) in the spectral range of 250 - 2100 nm at three angles of light incidence (65º, 70º and 75º) was used. Thickness and optical properties of obtained films were extracted from fitting of experimental data and modeled structure ones.

I-V (current-voltage) characteristics of SCs were studied in the darkness and under illumination with white light from tungsten halogen lamp with 136 mW/cm² intensity and IR filter to avoid sample heating.

II. Results and discussion
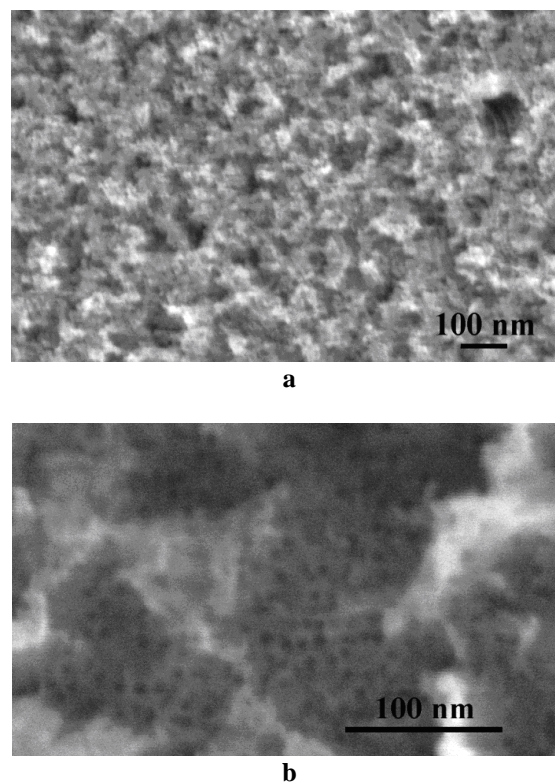
The initial layer of gold consists of individual 10-20

a

b

Fig. 3. SEM images of the surface of porous Si made by chemical etching initiated by gold nanoparticles before (*a*) and after (*b*) removal of gold nanoparticles.

nm in diameter nanoparticles as well as their aggregates on the slightly etched Si surface. SEM images of the surface of porous Si fabricated by metal assisted chemical etching before and after removal of gold nanoparticles are presented in Fig. 3. Porous Si layer obtained by this method had up to 200 nm thickness. Analysis of SEM images of the surface after chemical removal of gold (Fig. 3b) shows that the pores are cylindrical with a diameter of about 10-15 nm, separated and homogeneously distributed on the surface.

Reflectance spectra in Fig. 4 demonstrate that the reflection of light from the structures with porous layer is significantly reduced compared to the corresponding flat structures. Deposition of Au NPs on a flat polished Si leads to the minimum of reflection due to the excitation of local surface plasmon resonance in the region of 0.5 μm (curve 2). Numerical calculations based on effective medium approximation for composite media shows that thickness of metal films is about 10 nm and metal volume fraction $f \approx 0.14$. Metal-assisted etching of Si results in formation of porous layer on the surface of single crystal wafer. This porous layer is composite one because of Au nanoparticles are gradually sinking into Si below the surface level. Such porous composite layer on the surface of Si reveals an overall reduction in reflection (curve 3). The localized surface plasmon peak for Au NPs in composite becomes less pronounced. After etching and removal of Au NPs from Si pores the plasmon peak disappears but the total light reflection is decreased (curve 4) which is typical for porous rough surfaces.
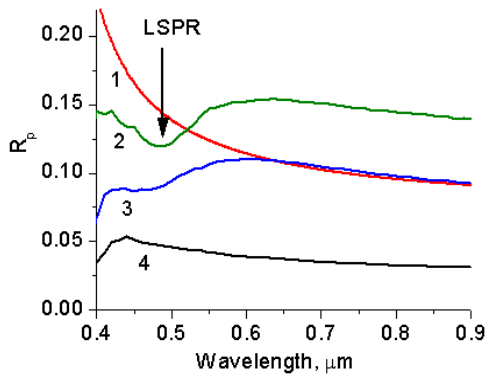
Fig. 4. Reflectance spectra of *p*-polarized light at incidence angle of 60° from: flat polished Si (curve 1), Si with deposited Au nanoparticles (curve 2), porous Si with Au nanoparticles (produced by MACE) (curve 3) and porous Si after removal of Au nanoparticles (curve 4). Arrow points out on local surface plasmon resonance (LSPR) excitation position in spectra.
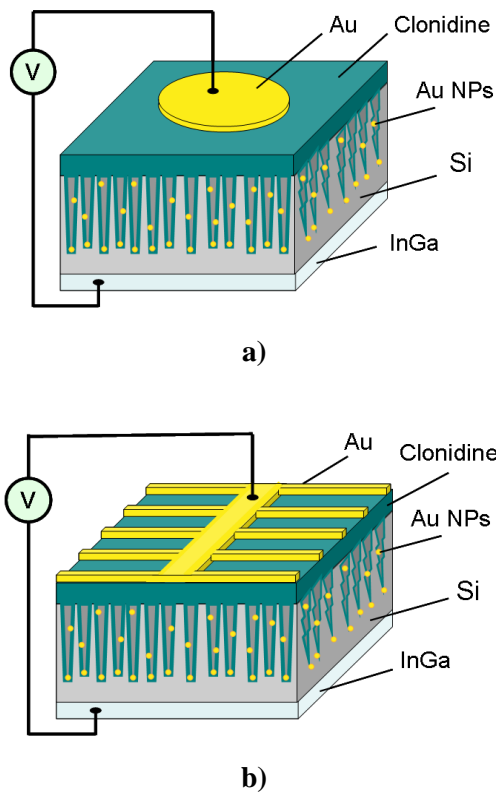

a)

b)

Fig. 5. Schematic representation of the construction of hybrid photodetector (*a*) and solar cell (*b*).

From spectroscopic ellipsometry investigations it was found that on the flat surface clonidine is deposited by a very thin layer of the order of 1 - 2 nm, which is only a few monolayers, thus probably forming chemical bonds with the silicon surface. Composite layers based on porous silicon are well described within the framework of a three-component approximation of an effective medium consisting of Si, clonidine and voids. The obtained thickness of the porous layer is 124 nm,

with the proportion of voids, Si and clonidine was 67 %, 6 % and 27 % respectively.

On the basis of the fabricated porous Si layer on the surface of *n*-Si wafer, heterojunctions with an organic clonidine film have been created (Fig. 5). The ohmic contacts were made by applying InGa alloy to the bottom of Si substrates. From the front side to the organic film the Au contact in the form of round diodes with a diameter of 1.3 mm (Fig. 5a), or a contact grid covered 16 mm^2 of surface with a thickness of ~50 nm was deposited by vacuum thermal evaporation to obtain SC (Fig. 5b). The light and dark current-voltage characteristics have shown that the structures have barrier properties and are suitable for the manufacture of solar cells.

The dark current-voltage characteristics of SC structures with and without clonidine, with and without Au nanoparticles for SCs are presented in Fig. 6. It can be seen that the presence of Au nanoparticles leads to an
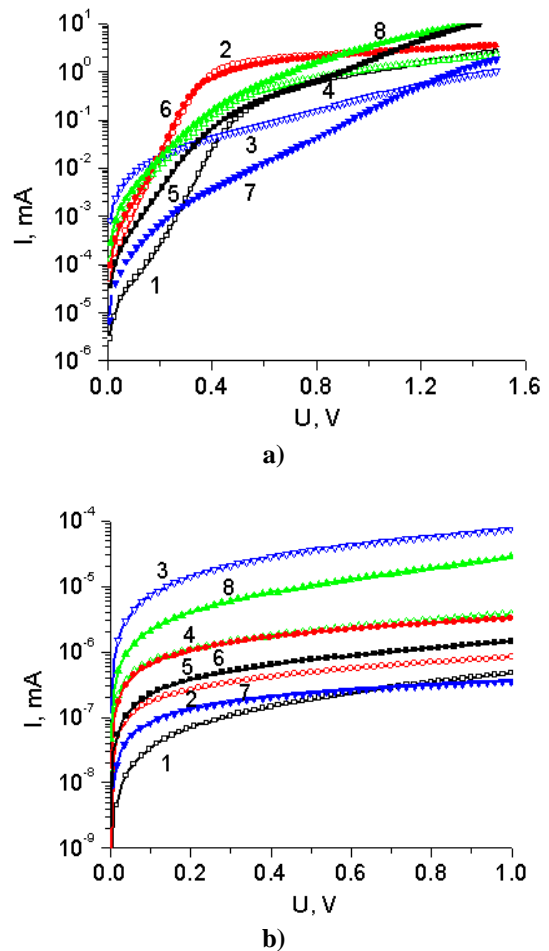

a)

b)

Fig. 6. Dark direct (*a*) and reverse (*b*) current-voltage characteristics of solar cells: flat structure (curve 1); flat structure with Au nanoparticles on the surface (curve 2); porous structure (curve 3); porous structure with Au nanoparticles in pores (curve 4); flat structure with clonidine film (curve 5); flat structure with clonidine film and Au nanoparticles on the surface (curve 6); porous texture with clonidine film (curve 7); porous texture with clonidine film and Au nanoparticles in pores (curve 8).

393

increase in the barrier (a higher voltage-current characteristic), an increase in the total current (due to an improved charge collection on the Si surface), a decrease in the series resistance (the curves are less saturated at high forward voltage values). Clonidine application also increases currents and decreases the series resistance on

SCs type structures.

The current-voltage characteristics have been analyzed by the method based on the determination of dimensionless sensitivity $DS = d \lg I / d \lg U$ [31-33]. Such approach gives peculiarities of current transport and injection mode in particular. Figure 7 shows the
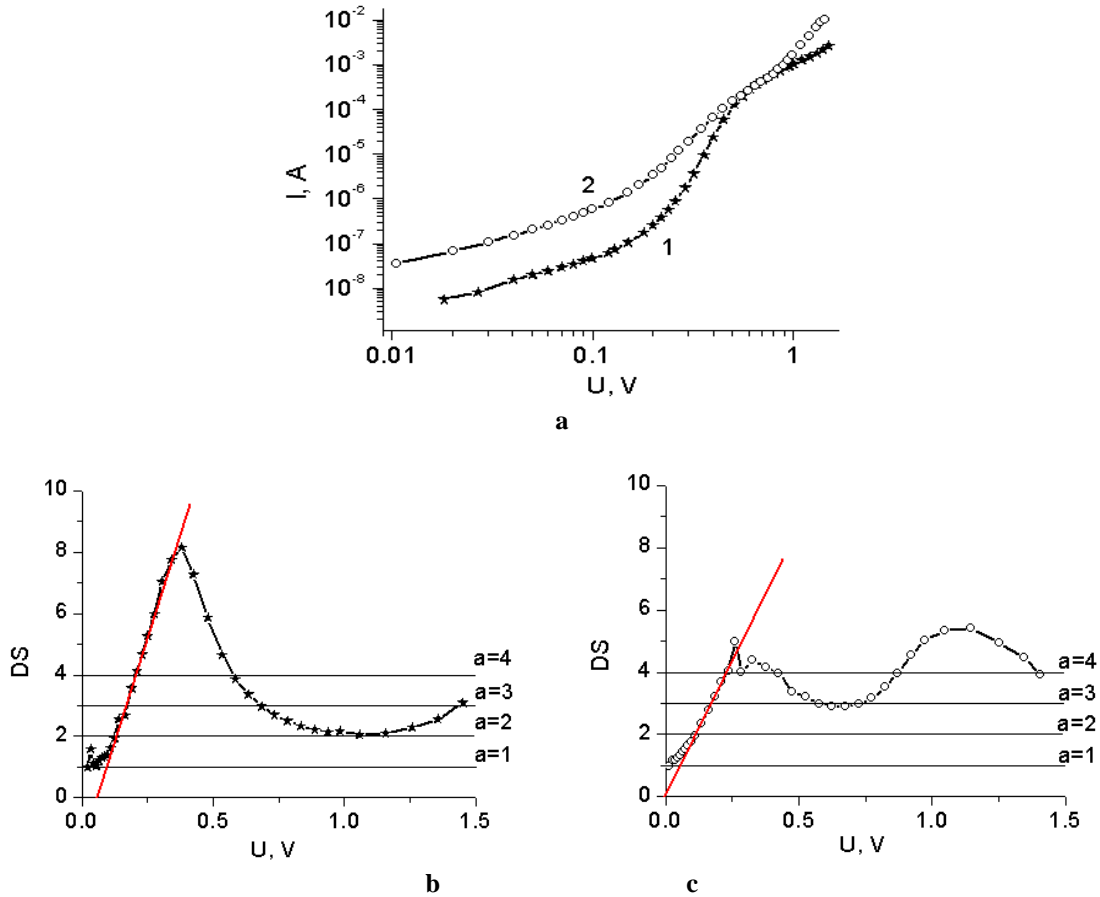

Fig. 7. Dark direct current-voltage characteristics of solar cells on the flat Si surface without (curve 1) and with clonidine film (curve 2) (*a*); *DS*(U) dependencies corresponding to curves 1 - (*b*) and 2 - (*c*).

Table 1

The dimensionless values of *DS* for the dark current-voltage characteristics of SCs on a flat and porous surface with and without gold and clonidine nanoparticles.

| DS value	Injection mode	Without clonidine	With clonidine	With gold nanoparticles on the surface	With gold nanoparticles and clonidine on the surface
Flat surface					
0.75	Current limitation by back contact			+	
1	Ohmic, contact restriction				+
2	Monomolecular recombination	+			
3	High injection rate		+		
4	Ultra-high injection rate		+		
Porous surface					
1.5	Bimolecular recombination			+	
3	High injection rate	+	No current restrictions		
4	Ultra-high injection rate				+
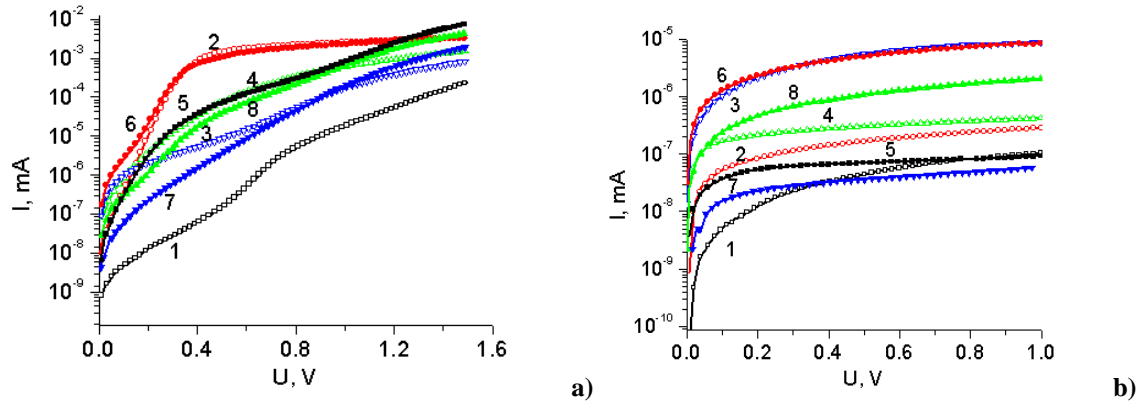
Fig. 8. Dark direct (*a*) and reverse (*b*) current-voltage characteristics of photodiodes fabricated on flat structure (curve 1); flat structure with Au nanoparticles on the surface (curve 2); porous structure (curve 3); porous structure with Au nanoparticles in pores (curve 4); flat structure with clonidine film (curve 5); flat structure with clonidine film and Au nanoparticles on the surface (curve 6); porous texture with clonidine film (curve 7); porous texture with clonidine film and Au nanoparticles in pores (curve 8).

Table 2

The dimensionless values of *DS* for the dark current-voltage characteristics of photodiode structures on a flat and porous surface without and with gold nanoparticles and clonidine.

S value	Injection mode	Without clonidine	With clonidine	With gold nanoparticles on the surface	With gold nanoparticles and clonidine on the surface
Flat surface					
0.75	Current limitation by back contact	No current restrictions		+	
1	Ohmic, contact restriction				+
3	High injection rate		+		
4	Ultra-high injection rate		+		
Porous surface					
0.75	Current limitation by back contact	No current restrictions	No current restrictions		No current restrictions
2	Monomolecular recombination			+	

experimental current-voltage characteristics and dependences of *DS(U)* for SCs fabricated on a flat Si surface with and without a clonidine film.

Processed by *DS* approach data for SCs are summarized in Table 1. They show that, on the flat surface, a clonidine layer promotes injection of current carriers, whereas a layer of gold nanoparticles on a flat surface, on the contrary, limits the current. There is no current limitation on the porous surface, in both cases.

The dark current-voltage characteristics of photodiode structures with clonidine and without clonidine, with and without Au nanoparticles are presented in Fig. 8. Processed by *DS* approach data for photodiodes are presented in Table 2. For this type structures, the use of Au nanoparticles and clonidine in principle results in the same effects, which reduces the shunt resistance by increasing the effective diode area because clonidine covers the entire sample surface with a solid film. Clonidine also significantly improves the

electrical performance of structures based on porous specimens, especially without Au nanoparticles.

Comparison of light current-voltage characteristics of solar cells and photodiode structures were performed at the identical for all structures AM0 conditions and gave that the most promising photovoltaic characteristics were achieved for photodiode type structures at simultaneous use of clonidine and Au nanoparticles (Fig. 9). The main parameters obtained from the current-voltage characteristics are shown in Table 3. In this case the increase of photocurrent and, as a consequence, the efficiency of solar cells and photodetectors is observed. A lot of factors are responsible for this effect such as: 1- improving barrier performance; 2 - the absorption of light around the heterojunction is increased due to the excitation of surface plasmons in Au nanoparticles; 3 - the conductivity of clonidine films is improved by transport through Au nanoparticles; 4 - clonidine film forms barrier contact with Si, where a lower barrier is
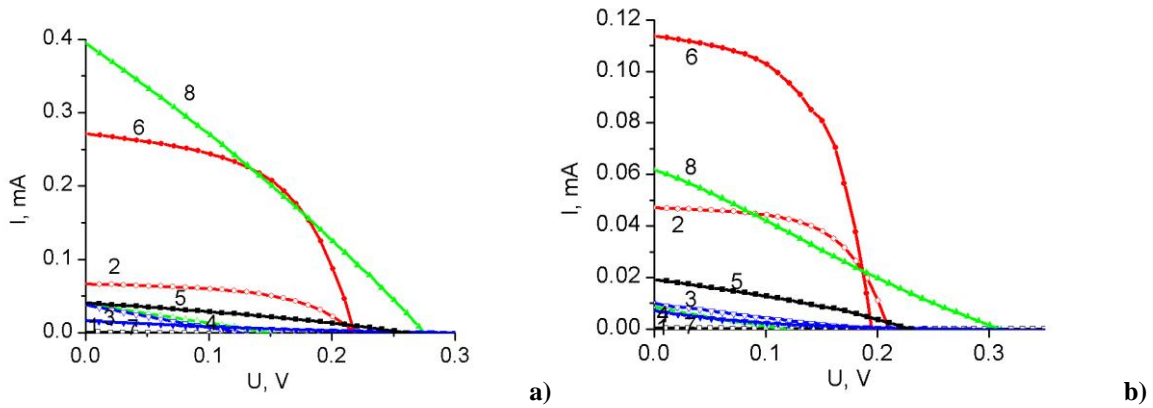
Fig. 9. Light current-voltage characteristics of solar cells (*a*) and photodiode structures (*b*) at AM0 conditions: flat structure (curve 1); flat structure with Au nanoparticles on the surface (curve 2); porous structure (curve 3); porous structure with Au nanoparticles in pores (curve 4); flat structure with clonidine film (curve 5); flat structure with clonidine film and Au nanoparticles on the surface (curve 6); porous texture with clonidine film (curve 7); porous texture with clonidine film and Au nanoparticles in pores (curve 8).

Table 3

Parameters of light current-voltage characteristics of solar cells

SC structure	Open circuit voltage U_{oc}, V	Short-circuit current I_{sc}, mA/cm^2	Fillfactor, f, %	Efficiency, η, %
Without clonidine				
Flat	0.045	0.005	26	<0.01
Flat + Au nanoparticles	0.218	0.417	52	0.03
Porous	0.126	0.236	24	0.01
Porous + Au nanoparticles	0.149	0.253	24	0.01
With clonidine				
Flat	0.259	0.254	31	0.01
Flat + Au nanoparticles	0.218	1.696	53	0.14
Porous	0.294	0.104	17	<0.01
Porous + Au nanoparticles	0.275	2.467	28	0.14

formed for holes than for electrons, which helps to separate photogenerated carriers and reduce recombination around the heterojunction.

It should be noted that in this work no special efforts were taken to reduce surface recombination, so the overall low efficiency values were obtained. These structures are modeled to determine the relative contribution of clonidine and metal plasmon-active nanoparticles to the photoconversion efficiency. It can be seen that the flat structure without clonidine and Au nanoparticles showed the worst characteristics, which is not surprising, since it is actually a Schottky barrier between the contact grid of Au and Si, which though has diode characteristics but very poorly collects charge from the Si surface which has low conductivity and high recombination. Therefore, it is preferable to make a comparison relative to flat structure with a clonidine film. For the last case, the additional use of Au nanoparticles increased the photocurrent by ~7 times, and the use of the porous composite layer added 1.5 times more.

In the further work it is worthwhile to optimize the thickness and composition of the composite films, to analyze the recombination losses in the obtained heterostructures in order to reduce them. It is necessary to solve the problem of high series resistance, which may be caused by the non-ideality of the ohmic contacts. Significant shunt resistance losses can also be reduced by removing edge effects. Separate research requires the stability of such SCs at the field testing conditions, at UV irradiation. Additional stability can be provided by the use of UV absorbing front transparent conductive films ZnO:Al, ITO, SnO$_2$:F, which at the same time it can improve the collection and transport of photogenerated carriers, and reduce the series resistance.

Conclusions

The technology of silicon nanoporation and fabrication of organics/inorganics heterojunctions for photodiode structures and solar cells have been developed. Microscopy studies have shown the porous structure of the films obtained and the presence of metal nanoparticles. The optical spectra reveal the excitation of surface plasmon modes in gold nanoparticles introduced

into composite porous layer. A study of the injection properties of barrier structures has shown that clonidine layer always promotes injection of current carriers, while gold nanoparticles limit photocurrent in the case of a flat surface. Photoelectric studies have shown an increase in photocurrent and the efficiency of the obtained photodetectors and solar cells due to the addition of both clonidine and Au nanoparticles. Thus, comparing to planar SC with clonidine, the additional use of Au nanoparticles increased the photocurrent by ~7 times, and the use of the porous structure by another 1.5 times.

Mamykin S.V. – Ph.D. in Phys.-Math. Sci., senior researcher, Head of the Department of Polariton Optoelectronics and Nanostructure Technology;
Mamontova I.B. – Ph.D. in Phys.-Math. Sci., researcher at the Department of Polariton Optoelectronics and Nanostructure Technology;

Kotova N.V. – junior researcher at the Department of Polariton Optoelectronics and Nanostructure Technology;
Kondratenko O.S. – Ph.D. in Phys.-Math. Sci., senior researcher at the Department of Polariton Optoelectronics and Nanostructure Technology;
Barlas T.R. – Ph.D. in Phys.-Math. Sci., senior researcher at the Department of Polariton Optoelectronics and Nanostructure Technology;
Romanyuk V.R. – Ph.D. in Phys.-Math. Sci., senior researcher at the Department of Polariton Optoelectronics and Nanostructure Technology;
Smertenko P.S. – Ph.D. in Phys.-Math. Sci., senior researcher, Head of the Electrophysical Diagnostics Group of Opto- and Microelectronics Structures, Laboratory of Physical and Technical bases of Optoelectronics;
Roshchina N.M. – Ph.D. in Techn. Sci., researcher at the Laboratory of Physical and Technical Bases of Optoelectronics.

[1] A. Fujishima, K. Honda, Nature 238(5358), 37 (1972) (https://doi.org/10.1038/238037a0).
[2] R. Zentel, Inorganics 8(3), 20 (2020) (https://doi.org/10.3390/inorganics8030020).
[3] S. Thomas, E.H.M. Sakho, N. Kalarikkal, O.S. Oluwafemi, J. Wu, Nanomaterials for Solar Cell Applications (Elsevier Science Publishing Co Inc, United States, 2019). ISBN: 978-0128133378.
[4] T. Dittrich, Nanocomposite Solar Cells. In book: Materials Concepts for Solar Cells, 2nd Edition (World Scientific Europe Ltd, United Kingdom, 2018), p. 383. ISBN: 978-1786344489 (https://doi.org/10.1142/9781786344496_0010).
[5] B. O'Regan, M. Grätzel, Nature, 353, 737 (1991) (https://doi.org/10.1038/353737a0).
[6] M. Grätzel, Photoelectrochemical cells. In book: Materials For Sustainable Energy: A Collection of Peer-Reviewed Research and Review Articles from Nature Publishing Group (Macmillan Publishers Ltd.: London, UK; World Scientific Publishing Co. Pte. Ltd.: Singapore, 2010), p. 26. ISBN 978-9814317641 (https://doi.org/10.1142/9789814317665_0003).
[7] A. Hagfeldt, M. Grätzel, Accounts of Chemical Research 33(5), 269 (2000) (https://doi.org/10.1021/ar980112j).
[8] C. Li, X. Yang, R. Chen, J. Pan, H. Tian, H. Zhu, X. Wang, A. Hagfeldt, L. Sun, Solar Energy Materials and Solar Cells 91(19), 1863 (2007) (https://doi.org/10.1016/j.solmat.2007.07.002).
[9] K. Hara, Y. Tachibana, Y. Ohga, A. Shinpo, S. Suga, K. Sayama, H. Sugihara, H. Arakawa, Solar Energy Materials and Solar Cells 77(1), 89 (2003) (https://doi.org/10.1016/S0927-0248(02)00460-9).
[10] S. Venkatesan, Q. Chen, E.C. Ngo, N. Adhikari, K. Nelson, A. Dubey, J. Sun, V. Bommisetty, C. Zhang, D. Galipeau, Energy Technology 2(3), 269 (2014) (https://doi.org/10.1002/ente.201300174).
[11] M.K. Siddiki, J. Li, D. Galipeau, Q. Qiao, Energy & Environmental Science 3(7), 867 (2010). (https://doi.org/10.1039/b926255p).
[12] Z.A. Peng, X. Peng, Journal of the American Chemical Society 123(1), 183 (2001) (https://doi.org/10.1021/ja003633m).
[13] D. Cui, J. Xu, T. Zhu, G. Paradee, S. Ashok, M. Gerhold, Applied Physics Letters 88(18), 183111 (2006) (https://doi.org/10.1063/1.2201047).
[14] S. Zhang, P. Cyr, S. McDonald, G. Konstantatos, E. Sargent, Applied Physics Letters 87(23), 233101 (2005) (https://doi.org/10.1063/1.2137895).
[15] V. Gernigon, P. Lévêque, C. Brochon, J.-N. Audinot, N. Leclerc, R. Bechara, F. Richard, T. Heiser, G. Hadziioannou, The European Physical Journal Applied Physics 56, 34107 (2011) (https://doi.org/10.1051/epjap/2011110150).
[16] J. Rud, L. Lovell, J. Senn, Q. Qiao, J. Mcleskey, Journal of materials science 40(6), 1455 (2005) (https://doi.org/10.1007/s10853-005-0582-2).
[17] Q. Liu, Z. Liu, X. Zhang, N. Zhang, L. Yang, S. Yin, Y. Chen, Applied Physics Letters 92(22), 223303 (2008) (https://doi.org/10.1063/1.2938865).
[18] M. Jørgensen, K. Norrman, S.A. Gevorgyan, T. Tromholt, B. Andreasen, F.C. Krebs, Advanced Materials 24(5), 580 (2012) (https://doi.org/10.1002/adma.201104187).
[19] G. Mariani, R.B. Laghumavarapu, B. Tremolet de Villers, J. Shapiro, P. Senanayake, A. Lin, B.J. Schwartz, D.L. Huffaker, Applied Physics Letters 97(1), 013107 (2010) (https://doi.org/10.1063/1.3459961).

[20] Ö. Güllü, A. Türüt, Solar Energy materials and Solar cells 92(10), 1205 (2008) (https://doi.org/10.1016/j.solmat.2008.04.009).

[21] S. Jäckle, M. Liebhaber, C. Gersmann, M. Mews, K. Jäger, S. Christiansen, K. Lips, Scientific Reports 7(1), 2170 (2017) (https://doi.org/10.1038/s41598-017-01946-3).

[22] Q. Liu, R. Ishikawa, S. Funada, T. Ohki, K. Ueno, H. Shirai, Advanced Energy Materials 5(17), 1500744 (2015) (https://doi.org/10.1002/aenm.201500744).

[23] D. Zielke, A. Pazidis, F. Werner, J. Schmidt, Organic-silicon heterojunction solar cells on n-type silicon wafers: The Back PEDOT concept, Solar Energy Materials and Solar Cells 131, 110 (2014) (https://doi.org/10.1016/j.solmat.2014.05.022).

[24] N.L. Dmitruk, O.Yu. Borkovskaya, I.M. Dmitruk, S.V. Mamykin, Z.J. Horvath, I.B. Mamontova, Applied Surface Science 190(1-4), 455 (2002) (https://doi.org/10.1016/S0169-4332(01)00918-7).

[25] I. Vangelidis, A. Theodosi, M.J. Beliatis, K.K. Gandhi, A. Laskarakis, P. Patsalas, S. Logothetidis, S.R.P. Silva, E. Lidorikis, ACS Photonics 5(4), 1440 (2018) (https://doi.org/10.1021/acsphotonics.7b01390).

[26] T.Ya. Gorbach, P.S. Smertenko, E.F. Venger, Ukrainian Journal of Physics 59(6), 601 (2014) (https://doi.org/10.15407/ujpe59.06.0601).

[27] S. Mamykin, A. Kasuya, A. Dmytruk, N. Ohuchi, Journal of Alloys and Compounds 434-435, 718 (2007) (https://doi.org/10.1016/j.jallcom.2006.08.121).

[28] M. Macherzynski, G. Milczarek, S. Mamykin, V. Romanyuk, A. Kasuya, Electrochimica Acta 55(14), 4395 (2010) (https://doi.org/10.1016/j.electacta.2010.02.008).

[29] Zh. Huang, N. Geyer, P. Werner, J. de Boor, U. Gösele, Adv. Mater. 23, 285 (2011) (https://doi.org/10.1002/adma.201001784).

[30] T.R. Barlas, M.L. Dmitruk, N.V. Kotova, O.I. Mayeva, V.R. Romanyuk. Superlattices and Microstructures 38, 130 (2005) (https://doi.org/10.1016/j.spmi.2005.04.003).

[31] R. Ciach, Yu.P. Dotsenko, V.V. Naumov, A.N. Shmyryeva, P.S. Smertenko, Solar Energy materials and Solar cells 76(4), 613 (2003) (https://doi.org/10.1016/S0927-0248(02)00271-4).

[32] P. Smertenko, L. Fenenko, L. Brehmer, S. Schrader, Advances in Colloid and Interface Science 116(1-3), 255 (2005) (https://doi.org/10.1016/j.cis.2005.05.005).

[33] G. Luka, L. Nittler, E. Lusakowska, P. Smertenko, Organic Electronics 45, 240 (2017) (https://doi.org/10.1016/j.orgel.2017.03.031).

С.В. Мамикін, І.Б. Мамонтова, Н.В. Котова, О.С. Кондратенко, Т.Р. Барлас, В.Р. Романюк, П.С. Смертенко, Н.М. Рощина

Нанокомпозитні сонячні елементи на основі гетеропереходу органіка/неорганіка (клонідин/Si) з плазмонними наночастинками Au

Інститут фізики напівпровідників ім. В.Є.Лашкарьова Національної академії наук України, Київ, Україна, mamykin@isp.kiev.ua

Методом селективного хімічного травлення, ініційованого металевими (золотими) наночастинками, були отримані плівки пористого кремнію на поверхні монокристалічних пластин. На таких підкладках осаджували ограничні плівки клонідину і виготовляли бар'єрні гетероструктури для отримання сонячних елементів та фотодіодів. Спектри відбиття світла підтвердили збудження локальної плазмонної моди в нанокомпозитах із золотими наночастинками. Фотоелектричні дослідження показали збільшення фотоструму сонячних елементів завдяки використанню як наноструктурованого кремнію, так і золотих наночастинок в 1,5 та 7 разів, відповідно. Вольт-амперні характеристики сонячних елементів на основі таких нанокомпозитів проаналізовані в термінах безрозмірної чутливості $DS = d\lg I / d\lg U$. Дослідження інжекційних властивостей структур показало, що шар клонідіну завжди сприяє інжекції носіїв струму, у той час як наночастинки золота обмежують струм у випадку плоскої поверхні.

Ключові слова: нанокомпозит; гетеропереходи органіка/неорганіка; кремній; золоті наночастинки; клонідин; інжекція електронів і дірок; безрозмірна чутливість; сонячні елементи.